The Second Int. Symp. on Turbulence and Shear Flow Phenomena, Vol. 2, pp. 175-180, Stockholm, 2001

A HYBRID LES–RANS MODEL BASED ON A ONE-EQUATION SGS MODEL AND A TWO-EQUATION $k-\omega$ MODEL

Lars Davidson
Dept. of Thermo and Fluid Dynamics
Chalmers University of Technology
SE-412 96 Göteborg, Sweden
http://www.tfd.chalmers.se/~lada, lada@tfd.chalmers.se

Shia-Hui Peng*
Dept. of Thermo and Fluid Dynamics
Chalmers University of Technology
SE-412 96 Göteborg, Sweden
http://www.tfd.chalmers.se/~peng, peng@tfd.chalmers.se

ABSTRACT

A hybrid LES-RANS model is proposed. RANS is used in the near wall regions ($y^+ \lesssim 60$), and the turbulence is modelled with a $k-\omega$ model. LES is used in the remaining part of the flow, and the SGS turbulence is modelled with a one-equation k_{sgs} model. The same continuity and momentum equations are solved throughout the domain, the only difference being that the turbulent viscosity is taken from the $k-\omega$ model in the RANS region, and from the one-equation k_{sgs} model in the LES region. The model is applied to two test cases, both incompressible: fully developed flow in a plane channel and the flow over a 2D-hill in a channel.

INTRODUCTION

Very fine grids must be employed in all three directions in Large Eddy Simulations. The near-wall grid spacing should be about $y^+ \simeq 1$ in the wall-normal direction which is similar to the requirement in RANS using low-Re number models. Contrary to RANS, a fine grid must also be used in the spanwise (z) and streamwise (x) directions in LES in order to resolve the near-wall turbulent structures in the viscous sublayer and the buffer layer(streaks), which are responsible for the major part of the turbulence production. The requirement for a well-resolved LES on Δx^+ and Δz^+ in the near-wall region is approximately 100 and 20, respectively.In the fully turbulent region, say for $y^+ > 50$, coarser grid spacing can probably be used; in this region Δx^+ and Δz^+ are presumably dictated by the requirement of resolving the mean flow rather than the near-wall turbulent processes.

In this work, we propose coupling a two-equation $k-\omega$ model in the near-wall region (RANS region) with a one-equation k_{sgs} model in the core region (LES region), see Fig. 1. The momentum equations are solved throughout the computational domain. The turbulent viscosity from the $k-\omega$ model is used in the RANS region, and the SGS viscosity from the one-equation model is used in the LES region. For simplicity, the matching line between the RANS and LES region is presently defined at a pre-selected grid line.

This approach is in a way similar to that used in DES (Detached Eddy Simulation) (Nikiton et al. 2000). One difference is that whereas in DES the object is to model the turbulent boundary layer with RANS; only the detached eddies in the outer boundary layer is modelled with LES. In the present hybrid LES-RANS, the matching line is located somewhere in the logarithmic part of the boundary layer.

THE HYBRID LES–RANS MODEL

A $k-\omega$ model (Peng et al. 1997) is used in the near-wall layer, the one-equation SGS model by Yoshizawa (1993) is used in the core

*Present address: FOI (Swedish Defence Research Agency), Aeronautics Division, SE-172 90 Stockholm

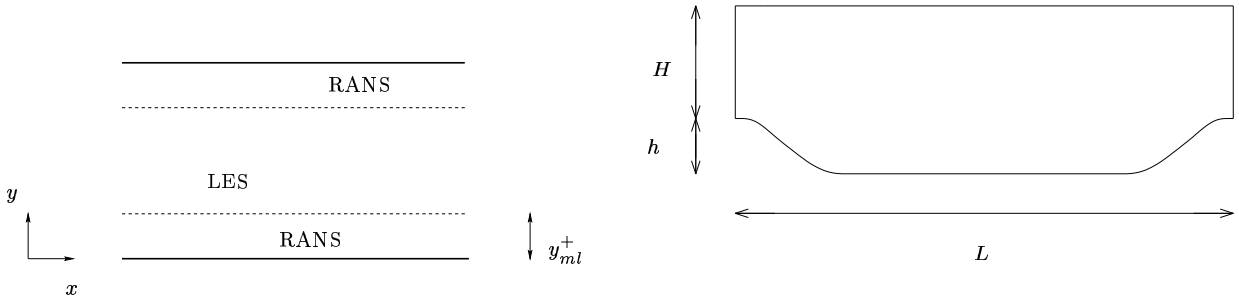

Figure 1: Left: The near-wall RANS region and the outer LES region; right: hill-flow configuration ($Re_b = U_b h/\nu \simeq 15\,800$, $\nu = 5 \cdot 10^{-6}$, $h = 0.028$, $H = 0.057$, $L = 9h$, $z_{max} = 9h$, U_b denotes the bulk velocity at the hill, i.e. $x = 0$ and $x = L$).

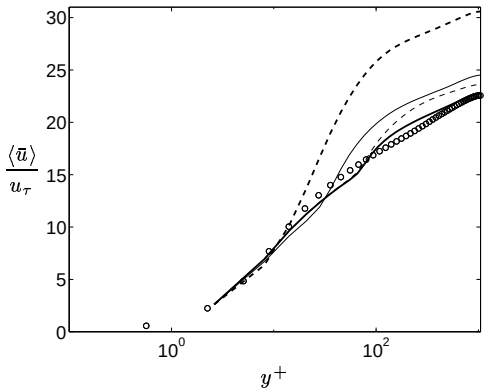

(a) Thin solid line: Case 1; thick solid line: Case 2; thin dashed line: Case 3; thick dashed line: Case 4.

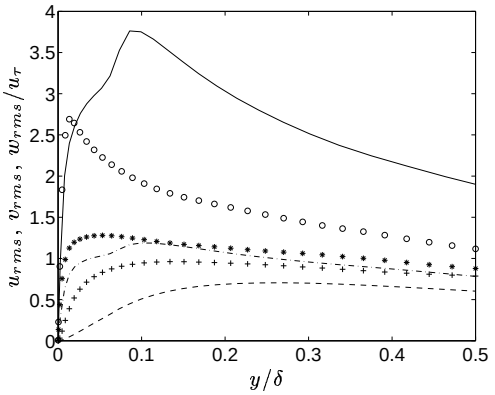

(b) Case 2. Resolved, rms fluctuations.

Figure 2: Channel flow. Markers: LES by Piomelli.

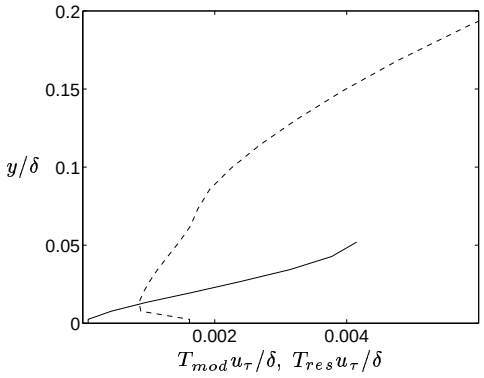

(a) Solid line: modelled turbulent time scale $u_\tau/(\delta\langle\omega\rangle)$; dashed line: resolved turbulent time scale $u_\tau\Delta/(\delta\langle k_{res}\rangle^{1/2})$.

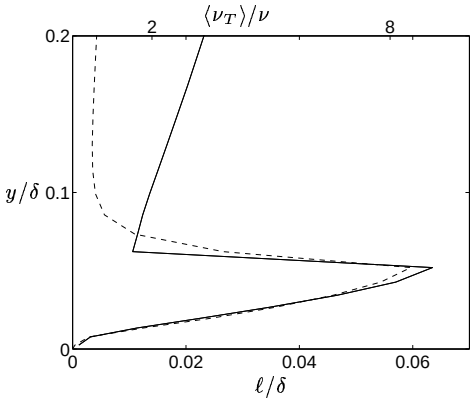

(b) Dashed line: turbulent/SGS viscosity. Solid line: turbulent/SGS length scales, $\ell = \langle \nu_T \rangle/(C_k \langle k_T \rangle^{1/2})$.

Figure 3: Channel flow, Case 2. Turbulent/SGS time and length scales, and turbulent/SGS viscosity.

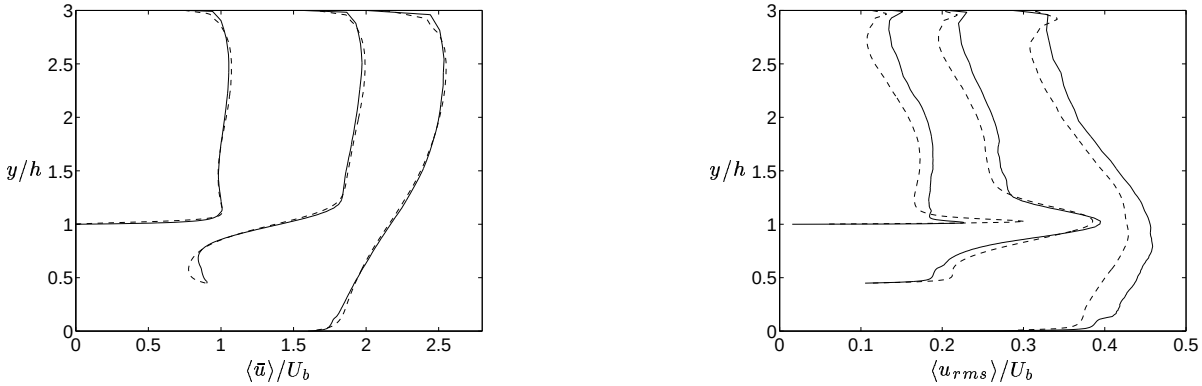

Figure 4: Hill flow. Profiles at $x = 0.005h, x = h, x = 6h$. Solid lines: hybrid LES-RANS; dashed lines: benchmark LES by Mellen et al.

Case	z_{max}	y_{ml}/δ	j_{match}	y^+_{ml}	Δz^+
1	π	0.023	4	25	104
2	π	0.057	8	60	104
3	2π	0.057	8	60	208
4	π	0	0	0	104

Table 1: Channel flow, $Re_\tau = 1050$, $x_{max} = 4\pi$ ($\Delta x^+ = 412$). Size of the computational domain and position of the matching line (y_{ml}) between the LES and RANS regions. The j_{match} value represents number of cells in the RANS region. Note that only LES is used in Case 4.

region. The model of Yoshizawa reads

$$\frac{\partial k_{sgs}}{\partial t}+\frac{\partial}{\partial x_j}(\bar{u}_j k_{sgs}) = \frac{\partial}{\partial x_j}\left[(\nu+\nu_{sgs})\frac{\partial k_{sgs}}{\partial x_j}\right] + P_{k_{sgs}} - C_\varepsilon \frac{k_{sgs}^{3/2}}{\Delta}$$
$$\Delta = \min\{\Delta_\xi, \Delta_\eta, \Delta_\zeta\},\ C_k = 0.07,\ C_\varepsilon = 1.05$$
$$P_{k_{sgs}} = 2\nu_{sgs}\bar{S}_{ij}\bar{S}_{ij},\ \nu_{sgs} = C_k \Delta k_{sgs}^{1/2} \quad (1)$$

where ξ, η and ζ denote the three coordinate directions defined by a general curvilinear grid. The coefficients have been assigned slightly different values (Fureby 1999) than in the original model. Note that, contrary to the standard Yoshizawa model, in which $\Delta = (\Delta_\xi \Delta_\eta \Delta_\zeta)^{1/3}$, we here use the smallest cell side, which was found to considerably improve the predictions.

The matching line near the lower wall is located at y_{ml}, see Fig. 1. Let j_{match} denote the cell below the matching line y_{ml}. The following boundary conditions are used At the matching line:

$$j = j_{match}:\ \frac{\partial k}{\partial y} = \frac{\partial \omega}{\partial y} = 0$$
$$j = j_{match}+1:\ \nu_{sgs,j_{match}+1} = \nu_{t,j_{match}}$$
$$\Rightarrow k_{sgs,j_{match}} = \left(\frac{\nu_t}{C_k \Delta}\right)^2_{j_{match}} \quad (2)$$

where ν_t denotes the RANS turbulent viscosity, and $k_{sgs,j_{match}}$ is the SGS kinetic energy that is transported by convection-diffusion over the matching line from the RANS region to the LES region. The boundary conditions at the interface presented above imply that k_{sgs} in the LES region is affected by k in the RANS region, but that k and ω in the RANS region are not influenced by k_{sgs} in the LES region.

NUMERICAL METHOD

An incompressible, finite volume code is used (Davidson 1997). For space discretization, central differencing is used for all terms. The Crank-Nicolson scheme is used for time discretization. The numerical procedure is based on an implicit, fractional step technique with a multigrid pressure Poisson solver and a non-staggered grid arrangement

RESULTS

For convenience, two quantities are here defined and used in the presentation below. For $y \le y_{ml}, \nu_T = \nu_t, k_T = k$, otherwise $\nu_T = \nu_{sgs}, k_T = k_{sgs}$.

Channel Flow

Figure 2a shows the predicted $\langle\bar{u}\rangle$ velocity ($\langle . \rangle$ denotes averaging over x, z and t) for fairly coarse meshes, see Table 1. A $32 \times 64 \times 32$ (x, y, z) grid is used. It can be seen that, for Case 2, in which the matching line is located at $y^+ = 60$, and $\Delta z^+ = 104$, the agreement with LES of Piomelli (1993) is quite good. However, a small kink is visible in the $\langle\bar{u}\rangle$ near the location of the matching line. When the resolution is made coarser in the spanwise direction (Case 3) the agreement with the benchmark LES becomes somewhat poorer. Note that the grid for Case 1, 2 & 3 is much coarser than that required for a wall-resolved LES. Consequently, when only LES is used (Case 4), the results are much poorer than those obtained with the hybrid LES–RANS model.

Figure 2b presents the predicted resolved, rms fluctuations. The agreement with benchmark LES is not very good. The predictions are typical of an under-resolved LES: the streamwise fluctuations are too large, and the wall-normal and spanwise fluctuations are too small. It should be noted that the resolved stresses are large even in the RANS region.

Hill Flow

The configuration of the hill flow is shown in Fig. 1. A $104 \times 64 \times 32$ (x, y, z) grid is used. The flow is periodic in both the streamwise and the spanwise directions. The matching line along the lower wall is fixed to grid line number 13, so that the location of the matching line is at $\langle n_{ml} \rangle / h = 0.1 \pm 0.02$. No RANS region is used along the upper wall, but the LES region extends up to the wall. The cell size in x and z together with the location of the matching line (all in wall units) are shown in Fig. 5. As can be seen, high local values in $\langle \Delta x^+ \rangle$ and $\langle \Delta z^+ \rangle$ occur above the crest, while $\langle \Delta x^+ \rangle \simeq \langle n_{ml}^+ \rangle \lesssim 30$ and $\langle \Delta z^+ \rangle \lesssim 100$ in the rest of the flow domain. For the nodes adjacent to the lower wall, $\langle y^+ \rangle \lesssim 2$. The predictions are compared with a benchmark LES (Mellen et al. 1999; Mellen et al. 2000) using more than 5 million cells.

Figure 4 compares the predicted $\langle \bar{u} \rangle$ velocity ($\langle . \rangle$ denotes averaging over z and t) and resolved, rms fluctuations with benchmark LES. The agreement is fairly good. As can be seen from the profile at $x = h$, the separation region with the hybrid LES-RANS model is slightly too strong. However, this is probably not due to the near-wall treatment, but it is believed to be a result of the shear layer emanating from the top of the hill not being sufficiently resolved. Small kinks are seen – hardly visible – in the $\langle \bar{u} \rangle$ profiles close to the location of the matching line. These kinks are much smaller than what was found in the channel flow (cf. Fig. 2). The reason is probably that, in the hill flow, the convective and diffusive transport across the matching line is considerable, which has a smoothening effect on the flow quantities.

Discussion

The turbulent/SGS viscosities are shown in Figs. 3b and 6a. It can be seen that in the RANS region, the turbulent viscosities are large in the RANS region – much larger than is normally found in LES. Near the matching line, ν_{sgs} in the LES region drops sharply down

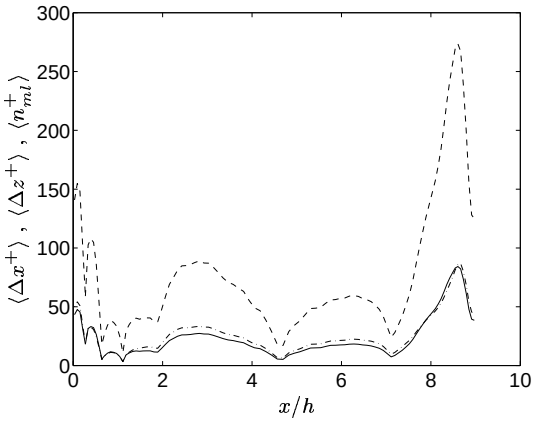

Figure 5: Hill flow. Grid spacing and location of matching line. Solid line: $\langle \Delta x^+ \rangle$; dashed line: $\langle \Delta z^+ \rangle$; dash-dotted line: $\langle n_{ml}^+ \rangle$.

to typical SGS values of $2 \leq \langle \nu_{sgs} \rangle / \nu \leq 4$. The maximum value of ν_t (Fig. 3b) in the RANS region, which occurs near the matching line, is $\langle \nu_{t,max} \rangle / \nu \simeq 9$. When 1D, steady RANS is used to compute the channel flow using the same grid and the same $k - \omega$ model, the value of ν_t at the same location is approximately twice as large. One of the reasons why the RANS calculation gives larger ν_t values than the hybrid LES-RANS, is that more modelled, turbulent, kinetic energy is generated in the former case in the outer part of the logarithmic region ($y^+ > 60$), which is transported towards the wall by turbulent diffusion. In the hybrid LES-RANS computations, the diffusion of modelled turbulence towards the wall is cut off at the matching line. Another reason is that in the hybrid LES-RANS computations, a substantial part of the turbulence in the RANS region is represented by resolved turbulence, see Fig. 2b.

Figures 3b and 7b give the modelled, turbulent length scales. The modelled turbulent/SGS viscosity can be defined as $\nu_T \propto \mathcal{U}\ell$, where $\mathcal{U}$ and ℓ represent a turbulent (SGS) velocity scale and length scale in the RANS (LES) region, respectively. In the LES region, the SGS length scale is $\ell = \Delta \equiv \nu_{sgs}/(C_k k_{sgs}^{1/2})$, see Eq. 1. In order to compare the turbulent and the SGS length scales, we define the turbulent length scale in the same way, so that $\ell = \nu_T/(C_k k_T^{1/2})$ in both the RANS and the LES region. As can be seen in Figs. 3b and 7b, the turbulent/SGS length scale decreases steeply from the RANS region to the LES region. Thus, the turbulent/SGS kinetic energy must increase to balance the decrease in the length scale in order to satisfy $\nu_{sgs} = \nu_t$, see Eq. 1. A large peak in k_{sgs} is created just out-

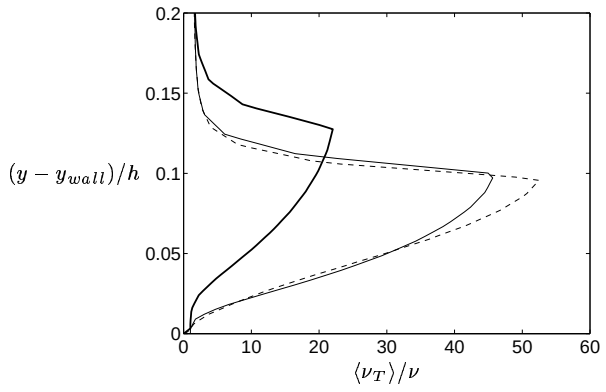

(a) Turbulent/SGS viscosity.

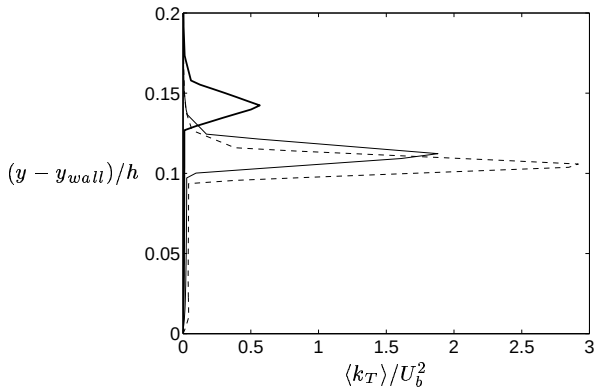

(b) Modelled turbulent/SGS kinetic energy.

Figure 6: Hill flow. Dashed line: $x/h = 0.005$; thick solid line: $x/h = 1$; thin solid line: $x/h = 6$.

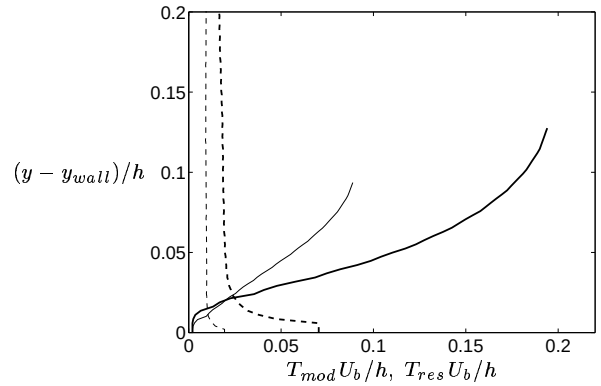

(a) Solid lines: turbulent modelled time scale $U_b/(h\langle\omega\rangle)$; dashed lines: resolved turbulent time scale $U_b\Delta/(h\langle k_{res}\rangle^{1/2})$. Thin lines: $x/h = 0.005$; thick lines: $x/h = 1$.

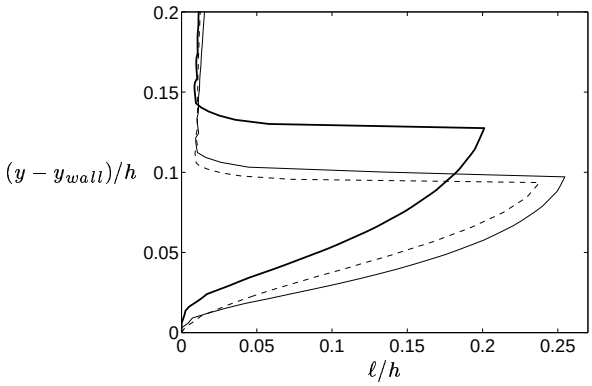

(b) Turbulent modelled length scale $\ell = \langle \nu_T \rangle / (C_k \langle k_T \rangle^{1/2})$. Dashed line: $x/h = 0.005$; thick solid line: $x/h = 1$; thin solid line: $x/h = 6$.

Figure 7: Hill flow.

side the matching line. The modelled SGS kinetic energy k_{sgs} in this region is of course not physical. This is not important, however, since the modelled quantity that enters the momentum equation is the turbulent/SGS viscosity ν_T, not k_T. The advantage of the condition $\nu_{sgs} = \nu_t$ across the matching line is that the gradient in the turbulent/SGS viscosity in the region of the matching line is reduced, because the gradient of k_T is smoothed out by convection/diffusion of k_T.

Davidson (2001) present predictions with an alternative condition at the matching line. No condition is set on either k_{sgs} or ν_{sgs}, but k is transported naturally from the RANS region to the LES region.

In unsteady RANS, there should be a scale separation between the modelled time scale, T_{mod}, and the resolved time scale, T_{res}, so that $T_{mod} \ll T_{res}$. In the RANS region, the turbulent viscosity is computed as $\nu_t = k/\omega$, and thus the modelled time scale can be defined as $T_{mod} = 1/\omega$. The highest resolved time scale is related to the resolved turbulence and the smallest length scale, and we define it as $T_{res} = \min\{\Delta_\xi, \Delta_\eta, \Delta_\zeta\}/\langle k_{res}\rangle^{1/2} = \Delta/\langle k_{res}\rangle^{1/2}$, where k_{res} is the resolved, turbulent kinetic energy. The modelled and the resolved time scales are compared in Figs. 3a and 7a and, as can be seen, the modelled time scale close to the wall is indeed smaller than the resolved one. However, in the larger part of the RANS region, the situation is the reverse: the modelled time scale is *larger* than the resolved one. Thus, formally, it is not correct to carry out an unsteady RANS. Indeed, it would be more correct to denote the near-wall region a VLES region rather than a RANS region. The SGS length scale in the VLES region is then $\ell = \nu_t/(C_k k^{1/2})$, which is presented in Figs. 3b

and 7b. Note that if we redefine the wall region from a RANS region to a VLES region, it does not have any implications for the finite volume code: *it remains the same.*

There may also be some question in defining the inner region as a VLES region. In this case, it may well happen that our SGS length scale, ℓ, becomes much larger than the filter size, Δ. Is that acceptable? It depends on *how* much larger. In Smagorinsky models, the SGS length scale is chosen as the cubic root of the cell volume, and this is much larger near walls than the smallest cell side. However, if the SGS length scale becomes *very much* larger than Δ, we may perhaps need to increase the filter size, i.e. do explicit filtering. This adds high complexity to the computations, especially since Δ would in general not be an even multiple of any cell width. A further complication would be that the SGS length scale – and also the filter width – would not be a function only of the space coordinates but also of time, i.e. $\Delta = \Delta(x_i, t)$. Thus there would be a commutation error in the time-derivative term in all equations, since the filter function is now a function of both space and time, i.e. $G = G(x_i, t)$.

CONCLUSIONS

The hybrid LES-RANS model has been applied to fully developed channel flow and the hill flow. The mean flow was fairly well predicted with a coarse mesh, both for the channel flow and the hill flow. Kinks in the velocity profiles were observed in the region of the matching line, but this problem was much smaller in the hill flow. The reason is probably that the transport of mass and momentum across the matching line by convection and turbulent diffusion, is much larger in the hill flow than in the channel flow, which reduce the kinks and sharp gradients in the region of the matching line. One way to further reduce the gradients across the matching line could be to use some kind of smoothing function as Strelets (2001) proposes, who is using a tanh function.

Acknowledgements

This work was financed by the LESFOIL project (no. BE97-4483) in the Brite-Euram programme. Computer time at the SGI ORIGIN 2000 machines at UNICC, Chalmers, is gratefully acknowledged.

References

Davidson, L. (1997). LES of recirculating flow without any homogeneous direction: A dynamic one-equation subgrid model. In K. Hanjalić and T. Peeters (Eds.), *2nd Int. Symp. on Turbulence Heat and Mass Transfer*, Delft, pp. 481–490. Delft University Press.[2]

Davidson, L. (2001). Hybrid LES-RANS: A combination of a one-equation SGS model and a $k - \omega$ model for predicting recirculating flows (to be presented). In *ECCOMAS CFD Conference*, Swansea, U.K.

Fureby, C. (1999). Large eddy simulation of rearward-facing step flow. *AIAA Journal 37*(11), 1401–1410.

Mellen, C., J. Fröhlich, and W. Rodi (1999). Karlruhe's mid-term report, LESFOIL: A Brite-Euram project. Technical report, Institut für Hydrodynamik, University of Karlsruhe, Germany.

Mellen, C., J. Frölich, and W. Rodi (2000). Large eddy simulation of the flow over periodic hills. In *16th IMACS World Congress 2000, Lausanne, August 21-25.*

Nikiton, N., F. Nicoud, B. Wasistho, K. Squires, and P. Spalart (2000). An approach to wall modeling in large-eddy simulations. *Physics of Fluids A 12*(7), 1629–1632.

Peng, S.-H., L. Davidson, and S. Holmberg (1997). A modified low-Reynolds-number $k-\omega$ model for recirculating flows. *ASME: Journal of Fluids Engineering 119*, 867–875.

Piomelli, U. (1993). High Reynolds number calculations using the dynamic subgrid-scale stress model. *Physics of Fluids A 5*, 1484–1490.

Strelets, M. (2001). Detached eddy simulation of massively separated flows. AIAA paper 2001–0879, Reno, NV.

Yoshizawa, A. (1993). Bridging between eddy-viscosity-type and second-order models using a two-scale DIA. In *9th Int. Symp. on Turbulent Shear Flow*, Volume 3, Kyoto, pp. 23.1.1—23.1.6.

[2] postscript file at http://www.tfd.chalmers.se/~lada